High precision, absolute total column ozone measurements from the Pandora spectrometer system: Comparisons with data from a Brewer double monochromator and Aura OMI

Maria Tzortziou,[1,2] Jay R. Herman,[2,3] Alexander Cede,[2,4] and Nader Abuhassan[2,5]

Received 22 March 2012; revised 15 June 2012; accepted 3 July 2012; published 22 August 2012.

[1] We present new, high precision, high temporal resolution measurements of total column ozone (TCO) amounts derived from ground-based direct-sun irradiance measurements using our recently deployed Pandora single-grating spectrometers. Pandora's small size and portability allow deployment at multiple sites within an urban air-shed and development of a ground-based monitoring network for studying small-scale atmospheric dynamics, spatial heterogeneities in trace gas distribution, local pollution conditions, photochemical processes and interdependencies of ozone and its major precursors. Results are shown for four mid- to high-latitude sites where different Pandora instruments were used. Comparisons with a well calibrated double-grating Brewer spectrometer over a period of more than a year in Greenbelt MD showed excellent agreement and a small bias of approximately 2 DU (or, 0.6%). This was constant with slant column ozone amount over the full range of observed solar zenith angles (15–80°), indicating adequate Pandora stray light correction. A small (1–2%) seasonal difference was found, consistent with sensitivity studies showing that the Pandora spectral fitting TCO retrieval has a temperature dependence of 1% per 3°K, with an underestimation in temperature (e.g., during summer) resulting in an underestimation of TCO. Pandora agreed well with Aura-OMI (Ozone Measuring Instrument) satellite data, with average residuals of <1% at the different sites when the OMI view was within 50 km from the Pandora location and OMI-measured cloud fraction was <0.2. The frequent and continuous measurements by Pandora revealed significant short-term (hourly) temporal changes in TCO, not possible to capture by sun-synchronous satellites, such as OMI, alone.

Citation: Tzortziou, M., J. R. Herman, A. Cede, and N. Abuhassan (2012), High precision, absolute total column ozone measurements from the Pandora spectrometer system: Comparisons with data from a Brewer double monochromator and Aura OMI, *J. Geophys. Res.*, *117*, D16303, doi:10.1029/2012JD017814.

1. Introduction

[2] The importance of ozone (O_3) in Earth's stratospheric and tropospheric chemistry, and its influence on radiative forcing and climate change, surface and underwater UV-B levels, local and regional environmental degradation, human health and vegetation, are well known, and have been discussed extensively in the literature [*Levy*, 1971; *Fishman et al.*, 1979; *Crutzen*, 1995; *Carpenter et al.*,1997; *Heck et al.*,1982; *Reich and Amundson*, 1985; *Diffey*, 1991; *Tevini*, 1993; *Chameides et al.*, 1994; *Environmental Protection Agency*, 1998; *World Health Organization*, 2000; *World Meteorological Organization*, 2006; *Intergovernmental Panel on Climate Change*, 2007; *Zerefos et al.*, 2009; *Herman*, 2010]. Meteorology and photochemical mechanisms involving various species of natural and anthropogenic sources (e.g., NO_x, CO, CH_4, VOCs, CFCs) have been shown to influence the formation, dispersion, destruction, and transport of O_3 in the atmosphere, often resulting in significant heterogeneities in O_3 distribution [*Fishman et al.*, 1979; *Comrie and Yarnal*, 1992; *Solomon*, 1999; *Tu et al.*, 2007; *Dueñas et al.*, 2002; *Lehman et al.*, 2004; *Crutzen*, 1995; *Crutzen et al.*, 1999; *Chameides*, 1978; *David and Nair*, 2011]. Nitrogen dioxide (NO_2) plays a critical role in these processes, as a major O_3 precursor in the lower troposphere and through catalytic destruction at higher altitudes [*Chameides*, 1978; *Logan et al.*, 1981; *Brasseur et al.*, 1998]. Simultaneous measurements of O_3 and NO_2 are, therefore, essential for improved understanding and predictive modeling of ozone photochemistry, distribution, and dynamics. Toward this objective, new ground-based spectrometer systems, Pandora, were recently

[1]Earth System Science Interdisciplinary Center, University of Maryland, College Park, Maryland, USA.
[2]NASA Goddard Space Flight Center, Greenbelt, Maryland, USA.
[3]Joint Center for Earth Systems Technology, University of Maryland, Baltimore County, Baltimore, Maryland, USA.
[4]LuftBlick, Kreith, Austria.
[5]School of Engineering, Morgan State University, Baltimore, Maryland, USA.

Corresponding author: M. Tzortziou, NASA Goddard Space Flight Center, Greenbelt, MD 20771, USA. (maria.a.tzortziou@nasa.gov)

0148-0227/12/2012JD017814

deployed at multiple sites in the U.S. (12), Europe (2) and Korea (2) for high temporal resolution, high precision, simultaneous measurements of various trace gases including O_3, NO_2, SO_2, BrO, water vapor and formaldehyde. Total column NO_2 retrievals from Pandora have been discussed in *Herman et al.* [2009] and shown to be of high precision (0.01 DU) and good accuracy ($\pm$0.05 DU). The purpose of this paper is to validate the capability of the Pandora spectrometer system to measure total column ozone (TCO) amounts compared to the widely accepted Brewer double monochromator throughout the day, and to the AURA-OMI satellite instrument during its overpass time.

[3] Ground-based measurements of TCO have been made during the past decades using a wide variety of instruments, including filter instruments and spectrometers. Dobson and Brewer spectrometers [*Dobson*, 1957; *Kerr et al.*, 1981; 1988] have been the most widely used, as they are the standard instruments for the Global Atmosphere Watch (GAW) program of the World Meteorological Organization, and remain one of the main sources of information about long-term ozone changes, trend analyses, and identification of possible natural or anthropogenic influences on atmospheric composition [*Loyola et al.*, 2009; *Fioletov et al.*, 2011]. In addition to TCO retrievals, Brewer measurements have been applied to retrievals of UV spectral measurements [e.g., *Lakkala et al.*, 2008], aerosol optical depth [e.g., *De Bock et al.*, 2010], total column SO_2 and NO_2 amounts [*Kerr et al.*, 1988; *Fioletov et al.*, 1998; *Cede et al.*, 2006b] and O_3 vertical distribution [*Tzortziou et al.*, 2008]. Dobson (starting in mid-1920s) and Brewer (developed in the late 1970s) instruments have a long history of ozone measurements that spans the data record for satellite retrievals (1979 to present) from TOMS, SBUV, SBUV-2, GOME, SCIAMACHY and OMI (Total Ozone Mapping Spectrometer, Solar Backscatter Ultraviolet, Global Ozone Monitoring Experiment, SCanning Imaging Absorption spectroMeter for Atmospheric CHartographY, and Ozone Monitoring Instrument) [*Bhartia et al.*, 1996, *Burrows et al.*, 1999, *Bovensmann et al.*, 1999; *Veefkind and de Haan*, 2002; *McPeters et al.*, 2008]. TCO retrievals for all instruments discussed here are based on the spectral fitting technique [see e.g., *Noxon*, 1975; *Platt et al.*, 1979], where the laboratory-measured absorption features of different species are fitted in the measured signals. Older instruments, such as Brewer, Dobson, TOMS, or SBUV use <10 channels (wavelengths), while newer instruments such as Pandora, SCIAMACHY and OMI use a much larger number of wavelengths in their retrievals. The Pandora TCO retrievals discussed in this paper use a variance weighted spectral fitting algorithm on the Pandora $\sim$0.6 nm spectral resolution direct-sun radiance measurements in the spectral range 310–330 nm, after correction for stray light effects.

[4] Improved understanding of small-scale atmospheric dynamics and spatial heterogeneities in trace gas distribution through ground-based observations require measurements at high spatial and temporal resolution. The small size and portability of the Pandora spectrometer system allow deployment at multiple sites within an urban air-shed, and development of a ground-based monitoring network for studying trace gas dynamics, local pollution conditions, photochemical processes and interdependencies of ozone and its major precursors. Such information is also critical for validation of satellite trace gas retrievals under a wide variety of conditions [*Herman et al.*, 2009].

[5] In this paper we present high temporal resolution measurements of absolute total column ozone amounts derived from the Pandora spectrometer. For the first time, ozone retrievals are routinely performed using a high-resolution extraterrestrial spectrum derived from independent measurements as the reference spectrum. The spectrum used is the *Kurucz* [2005] spectrum that is radiometrically corrected to the Atlas-3 SUSIM spectrum (M. E. Van Hoosier, The ATLAS-3 solar spectrum, 1996, available at ftp://susim.nrl.navy.mil/pub/atlas3) as described in *Bernhard et al.* [2004]. Convolution of the Kurucz spectrum to the Atlas-3 SUSIM resolution enables the removal of a small radiometric variation in the Kurucz spectrum that could masquerade as an atmospheric absorber if uncorrected. The result is a radiometrically corrected Kurucz spectrum with very high wavelength accuracy (picometer) and an estimated radiometric offset accuracy of 3% [*Thuillier et al.*, 2003]. The corrected high-resolution spectrum was then convoluted with the Pandora slit function to be used as a top-of-the atmosphere (TOA) reference spectrum. This method is very different from the usual technique of using a TOA reference spectrum based on the instrument's own measurements from a Langley extrapolation to zero air mass [e.g., *Herman et al.*, 2009]. Using the independent spectrum technique gives an absolute measurement of TCO, since the reference spectrum is free of residual atmospheric absorption. The method requires an accurate knowledge of the instrument's slit function as determined in the laboratory, but is insensitive to a radiometric calibration offset that only changes smoothly with wavelength. For example, a change that can be fit with a 4th order polynomial.

[6] Results are presented for four mid- (i.e., 39°N) to high- (i.e., 65°N) latitude sites where different Pandora instruments (one CMOS system #9, and two CCD systems #2 and #21) were used: GSFC (Goddard Space Flight Center), in Maryland U.S., where the longest Brewer and Pandora collocated data records have been available (June 2009 to September 2010); Cabauw in the Netherlands,where measurements were obtained as part of the CINDI (Cabauw Intercomparison Campaign of Nitrogen Dioxide measuring Instruments) campaign during June–July 2009 [*Roscoe et al.*, 2010]; Helsinki in Finland (September–October 2011); and Fairbanks in Alaska, where observations were performed as part of a large field campaign focusing on trace gas measurements at high latitudes (March–April 2011). Comparisons between Pandora, our ozone network double-grating Brewer spectrometer (#171), and Aura-OMI satellite retrievals are discussed.

2. Methods

2.1. Pandora Technical Characteristics

[7] The Pandora spectrometer system consists of a head sensor with foreoptics, mounted on a computer controlled sun-tracker and sky-scanner ($\sim$0.01° pointing precision), and connected to an array spectrometer by means of a 400 micron single strand multimode optical fiber (Figure 1). A drawing of the head sensor is shown in Figure 2. To achieve wavelength and radiometric calibration stability, the spectrometer is temperature stabilized inside an insulated enclosure using an actively coupled thermo-electric cooler and

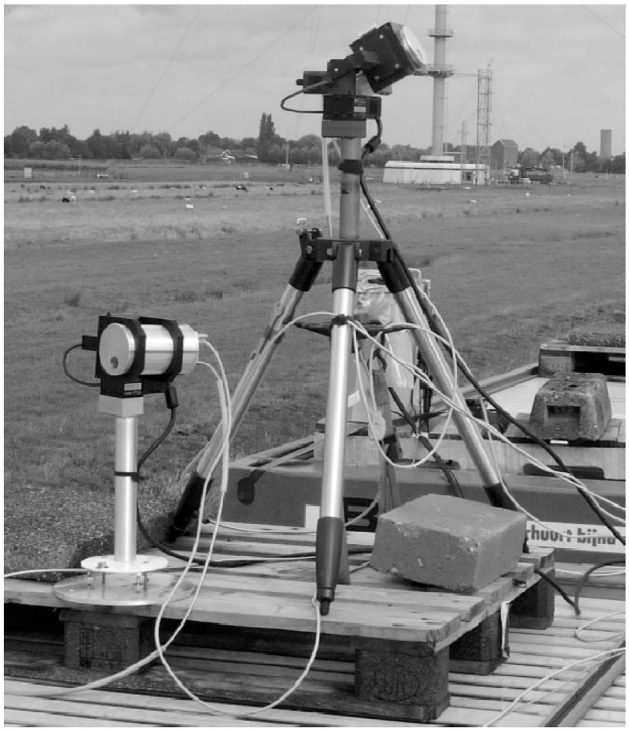

Figure 1. Sky-radiance plus direct-sun Pandora CCD spectrometer system (left) and direct-sun only Pandora CMOS spectrometer (right) in Cabauw.

heater. A detailed description is given in *Herman et al.* [2009].

[8] There are two versions of the Pandora spectrometer system, the Sun-only CMOS detector Pandora and the CCD detector Sun-and-Sky Pandora (Table 1). The CMOS Pandora spectrometer system operates only in direct-sun observation, as it is not sensitive enough to measure sky radiances. The CCD version is about 10^4 times more sensitive (partly from the detector and partly from the addition of a lens to focus light on the optical fiber) and detects sky radiances easily. The CMOS head sensor is similar to the CCD version shown in Figure 2, but without the lens and the first filterwheel. Baffles are used to produce a purely geometrical field of view (FOV) of about 1.6° full width half maximum (FWHM), which is independent of wavelength. It uses an Avantes spectrometer with a 1024 pixel detector (Table 1). The Sun-and-Sky Pandora spectrometer system (Figures 1 and 2, Table 1) uses the head sensor as shown in Figure 2 and an Avantes spectrometer with a UV sensitive back-thinned 2048 × 16 pixel CCD. The neutral density filters (ND1, ND2, ND3, and ND4) in the first filterwheel give a 10,000:1 dynamic range, which combined with the exposure range 4–4000 ms gives an overall dynamic range of 10^7 needed for sun and sky observations at all latitudes and seasons. The 1.5° FOV of the Sun-and-Sky Pandora is produced by the lens and baffles with a small measured wavelength dependence. The Brewer FOV (2.6°) is larger than the Pandora FOV (~1.5°). Wavelength calibration and slit functions for the Pandora instruments

Table 1. Sun-Only CMOS and Sun-and-Sky CCD Detector Pandora Characteristics

	Sun-Only CMOS	Sun-and-Sky CCD
Wavelength Interval	280 to 500 nm	280 to 525 nm
Spectral resolution	0.6 nm	0.6 nm
Oversampling	2.3 pixels	4.2 pixels
Detector	CMOS 1024 pixels	2048 pixels backthinned CCD
Field of view	1.6°FWHM	1.6°FWHM
Pointing Precision	0.01°	0.01°
Neutral Density Filter	None	ND1 to ND4

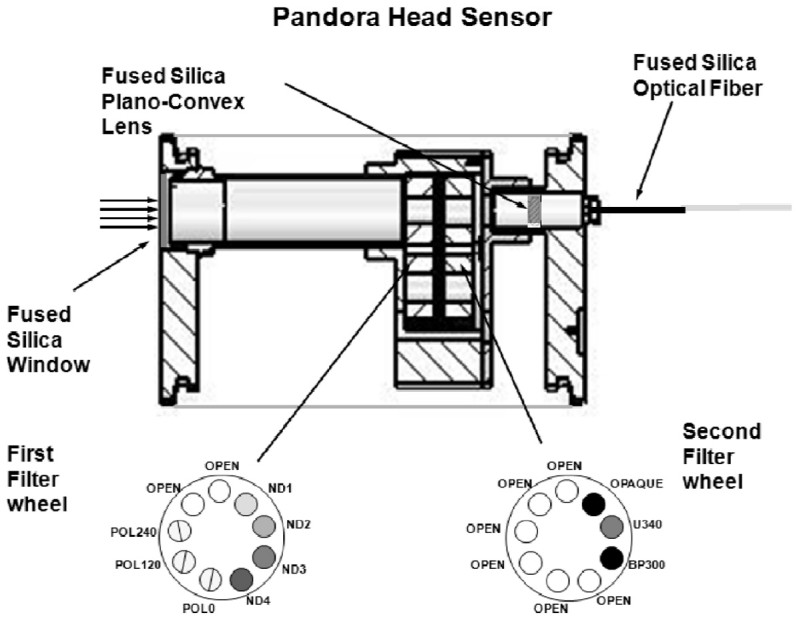

Figure 2. Schematic of internal optics of the Pandora head sensor.

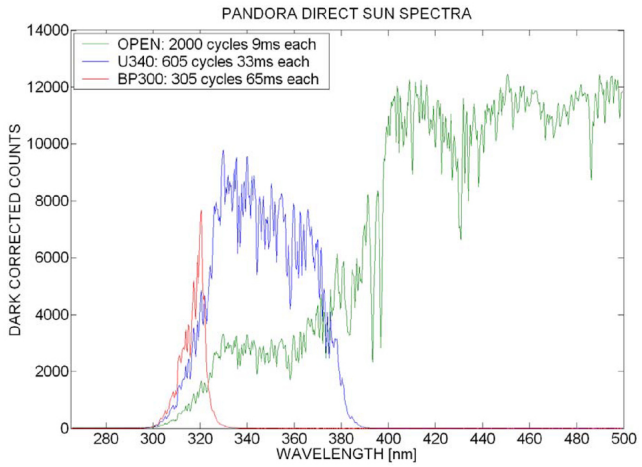

Figure 3. The direct sun spectrum measured by Pandora using open hole (green), a U340 filter (blue), and the BP300 filter (red).

are determined from lamp emission lines (Hg, Cd, Cu, In, Mg, Zn). Wavelength stability is validated during field use by an analysis of the solar Fraunhofer line structures.

[9] Accurate measurements of TCO amounts in the 310 to 330 nm range require a correction for the stray light effect, which is reduced by using UV band pass filters. Pandora instruments use two UV band pass filters, BP300 (280–320 nm) and U340 (280–380 nm) with cutoffs at 320 and 380 nm, respectively. The effect of the filters on the spectra is shown in Figure 3 compared to the spectrometer response to the solar spectrum using an open hole in the filterwheel. A stray light correction (see section 3) is obtained using the signal on the detector from wavelength positions less than 290 nm where the incident sunlight is nearly zero.

2.2. Pandora Total Ozone Spectral Fitting Algorithm

[10] Here we analyze TCO amounts from Pandora operated in direct-sun viewing mode. The spectral fitting algorithm uses laboratory measured absorption cross sections for each atmospheric absorber (i.e., O_3, NO_2, SO_2, HCHO, BrO for the 310–330 nm spectral region used here), a 4th order polynomial in wavelength to remove aerosols and Rayleigh scattering effects, and wavelength shift and squeeze functions. The shift and squeeze functions provide the best match to the measured spectrum compared to a solar reference spectrum containing the solar Fraunhofer line structure [*Herman et al.*, 2009]. High resolution O_3 cross sections [*Daumont et al.*, 1992], at a nominal effective ozone temperature of T = 225°K, were used in our retrievals. The effects of local and seasonal temperature changes on the O_3 cross sections and TCO retrievals are discussed in section 3.

[11] The approach of using the independently measured *Kurucz* [2005] ground-based extraterrestrial spectrum, normalized to Atlas Susim-3, avoids the errors associated with performing a Langley extrapolation [e.g., *Gröbner and Kerr*, 2001; *Bais*, 1997] of the Pandora measured solar spectrum to zero air mass. The Langley extrapolation method, used by the Brewer, usually has to be made at a very clean atmospheric site such as Mauna Loa, Hawaii under the assumption that ozone is constant as a function of solar zenith angle (air mass). The resulting calibration can be transferred to other Brewer instruments, which then measure ozone relative to the transfer instrument.

2.3. Brewer Total Ozone Retrieval

[12] In its various versions, the Brewer spectrometer has been available since the 1980s for measurements of solar irradiance and zenith sky radiances, which can then be used to derive total column O_3, SO_2, and NO_2 amounts [*Kerr et al.*, 1981, 1985, 1988; *Fioletov et al.*, 1998; *Cede et al.*, 2006b]. Most Brewers are single monochromators, but a number of systems are double monochromators with the advantage of a very low internal stray light fraction ($<10^{-7}$) at the short UV-B wavelengths enabling high accuracy measurements even at high solar zenith angles (SZA).

[13] The very low instrumental stray light makes the Mark III Brewer ideal for measuring Rayleigh scattered sky radiances in the UV spectral region except for the problem of polarization sensitivity related to the grating and to the flat quartz entrance window (Fresnel effect) covering the entrance port [*Cede et al.*, 2006a]. To eliminate both sources of polarization sensitivity so that accurate sky radiances can be obtained in the presence of aerosols, we have modified our Mark III Brewer instrument (#171) by introducing a depolarizer in front of the grating and by installing a curved quartz window such that the incident radiances observed by the spectrometer are always perpendicular to the window surface. Sky radiance measurements from Brewer #171 have been applied successfully to retrievals of O_3 vertical distribution [*Tzortziou et al.*, 2008]. For total column amount retrievals of ozone and other trace gases such as SO_2 and NO_2, the modified Brewer system at Goddard has been used in direct-sun viewing mode.

[14] The Brewer TCO retrievals are based on the Bass and Paur ozone absorption coefficients at a constant temperature of 228.3 K [*Bass and Paur*, 1985] that were modified by *Kerr* [2002]. TCO amounts were estimated here by using both the operational 4- and the 6-wavelength Brewer algorithms. In the operational algorithm the intensity of direct sunlight at the Brewer 4 longest wavelengths, 310.1, 313.5, 316.8 and 320 nm, are used to calculate column ozone. A set of fixed weighting coefficients is applied, chosen to minimize the effect of SO_2, temperature sensitivity, small wavelength shifts, and to suppress variations that change linearly with wavelength [*Kerr et al.*, 1981, *Kerr*, 2002; *Fioletov et al.*, 2005; *Petropavlovskikh et al.*, 2011]. In the Brewer 6-wavelength algorithm, two additional wavelengths at 303 and 306 nm are used to calculate TCO, which enhances the retrieval sensitivity to ozone changes [*Redondas and Cede*, 2006]. However, the decrease in the signal at 303 and 306 nm with increasing SZA requires use of SZA-dependent weights in the 6-wavelength algorithm, such that at high SZA, 303 and 306 nm get low weights and the 6-wavelength algorithm is approximately reduced to the operational algorithm. Because of the relatively strong stray-light contribution in the 303–306 spectral region, the 6-wavelength TCO retrieval is not recommended for measurements using a Brewer single spectrometer.

[15] In the Brewer, there are 6 wavelengths in slit-mask mode, which are measured nearly simultaneously (0.1147 s per wavelength) reducing the influence of changing sky

conditions compared to classical wavelength scanning instruments (rotating grating). The Pandora system measures all wavelengths simultaneously, so that it has no "noise" introduced from changing sky conditions during a measurement. Although the Pandora instrument noise at a single wavelength is comparable to, or higher, than the Brewer, the noise effect in Pandora is minimized by using many more wavelength samples (80 for the CMOS, 2× oversampled, and 160 for the CCD, 4× oversampled, spectrometers in the 310 and 330 nm spectral region), compared to 4–6 for the Brewer with no oversampling, and by time averaging (up to 200 individual measurements for the CMOS and 4000 for the CCD per 20 s). For example, at SZA = 70°, the Brewer noise at 310 nm (∼0.7%) is better than the Pandora noise at 310 nm (∼3%), while at 320 nm both instruments have about the same noise level (∼0.4%). Similarly to the Brewer 6-wavelength algorithm, the Pandora algorithm weights the importance of the wavelengths inversely with the measured noise variance, so that as the SZA increases the importance of the short wavelengths decreases. Pandora stray light is comparable to single Brewer at about 1×10^{-5} when normalized to 1 at the peak signal at each wavelength. However, the use of UV band-pass filters significantly reduces the stray light effect in Pandora (see section 3.1).

2.4. Study Sites and Instrumentation

[16] *Greenbelt, Maryland:* Measurements of TCO from our modified Mark III Brewer double monochromator (#171) and a collocated Pandora CMOS spectrometer (#9) were performed on the roof of a building, about 88 m above sea level, at GSFC in Greenbelt, MD (Lat = 38.993°N, Long = 76.840°W). The Brewer instrument was operating at GSFC from November 2000 to September 2010, providing a long time series of trace gas and aerosol amounts. Measurements from the Pandora CMOS instrument used in this study have been performed at this site since spring 2009. GSFC is a moderately polluted site, in the Baltimore-Washington DC metropolitan area. High ozone in the boundary layer is typically observed during April-September, particularly during the summer months [*Maryland Department of the Environment (MDE)*, 2008]. The site is located close to two major highway systems that are strong sources of NO_x emissions resulting in high inhomogeneity and rapid changes in local tropospheric composition [*Herman et al.*, 2009].

[17] *Cabauw, Netherlands:* Total column ozone and trace gas retrievals by the Pandora #9 CMOS spectrometer were also performed at KNMI's Cabauw Experimental Site for Atmospheric Research (CAESAR) in the Netherlands (Lat = 51.970°N, Long = 4.926°E), during June–July 2009. Cabauw is a rural site, approximately 50 km from the North Sea and surrounded by densely populated and industrialized areas (33 km NE of the city of Rotterdam and 30 km SW of Utrecht). The climate in the area is characterized as a "moderate maritime" with a prevailing southwesterly circulation and precipitation spread over the seasons. Atmospheric conditions are characterized by large variability, ranging from very clean maritime to highly polluted air masses. Our measurements were part of the Cabauw Intercomparison Campaign of Nitrogen Dioxide measuring Instruments (CINDI campaign) [*Piters et al.*, 2012]. Weather conditions during the campaign were mixed, with frequent changes in cloud cover, some rainy periods, and some early morning mist [e.g., *Roscoe et al.*, 2010; *Zieger et al.*, 2011]. Apart from NO_2, other measured and intercompared parameters included aerosol, HCHO, O_2O_2, CHOCHO, and BrO. The campaign was held under the auspices of the European Space Agency (ESA), the international Network for the Detection of Atmospheric Composition Change (NDACC), and the EU Framework 6's ACCENT-AT2 Network of Excellence and GEOMON Integrated Project.

[18] *Fairbanks, Alaska:* Trace gas measurements by two Pandora instruments (the #9 CMOS and the #2 CCD systems) and the Brewer double monochromator (#171) were performed in Fairbanks Alaska (Lat = 64.820°N, Long = 147.870°W) during March and April 2011, as part of a large field campaign focusing on measurements of total column BrO, NO_2 and O_3, and ozone vertical distribution at high latitudes. As part of this campaign, O_3 and NO_2 amounts were obtained and compared to the Brewer double monochromator (#171). All instruments were located on the roof of a building at the University of Alaska Fairbanks campus, with a clear view of the morning sun horizon. The conditions during the campaign contained days that were mostly free of clouds (24, 25, 31 March and 1, 9, 11 April), some with light cloud cover (26, 27 March and 2 April), and the rest with moderate to heavy cloud cover. Both NO_2 and O_3 data can be obtained by Pandora on days with light cloud cover, but with increased noise caused by the reduced number of measurements per 20 s.

[19] *Helsinki, Finland*: Measurements from another Pandora CCD system (#21) are reported for Helsinki, Finland (Lat = 60.204°N, Long = 24.961°E). Observations have been performed as part of a campaign that started in September 2011 to demonstrate the instrument's performance at high SZA and to measure trace gases at high latitudes (NO_2, O_3, HCHO and BrO). The location of the instrument is on top of the Finnish Meteorological Institute (FMI), in an area of moderate automobile traffic with frequent maritime and occasional polluted air masses.

3. Results and Discussion

3.1. Ground-Based Instrument Intercomparison: Pandora and Brewer

[20] To examine the Pandora performance over a relatively long data record, TCO retrievals from Pandora instrument #9 were compared with measurements derived from the double-grating Brewer monochromator #171 at the GSFC site during June 2009 to September 2010 (Figures 4–6). Because of the higher frequency in Pandora measurements, the Pandora data were interpolated to Brewer measurement times, using only observations that were closer than 5 min apart. Pandora measurements were filtered for normalized root-mean square (RMS) of weighted spectral fitting residuals less than 0.05 and estimated error in TCO less than 2 DU. Similarly, the Brewer measurements were filtered for standard error in TCO less than 2 DU. In addition, Brewer measurements were filtered for cloud and aerosols optical depth at 320 nm less than 1.0.

[21] Comparisons at GSFC are shown between Pandora and Brewer for the 6-wavelength (6w) Brewer TCO retrievals (Figure 4a). Similar results were obtained for the operational (Op) 4-wavelength algorithm, although the Brewer and Pandora agreement was slightly better for the 6w-algorithm.

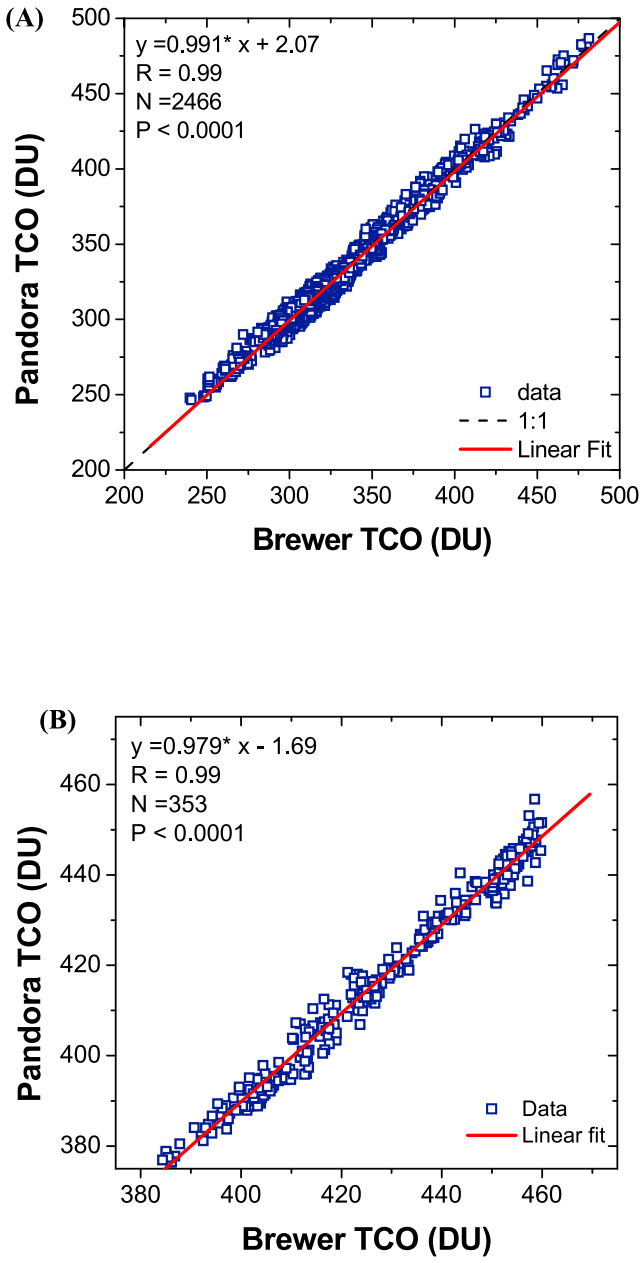

Figure 4. Comparison between TCO measurements from (a) Pandora (instrument #9) and the Brewer double-grating spectrometer (#171), collocated at the GSFC site, using the 6-wavelength Brewer TCO algorithm. (b) Pandora (instrument #2) and the Brewer double-grating spectrometer (#171) in Fairbanks Alaska during March–April 2011.

In both cases, the Pandora versus Brewer estimated least squares straight line fit was almost a perfect 1:1 within the standard deviation of the least squares fit (Slope = 0.987, Offset = 2.65 DU, R = 0.99, N = 2466, P < 0.0001 for the Op-algorithm; Slope = 0.991, Offset = 2.07 DU, R = 0.99, N = 2466, P < 0.0001 for the 6w-algorithm). The good agreement in accuracy over a wide range of ozone values (240–490 DU) suggests that the Brewer transferred Mauna Loa calibration and the absolute calibration of Pandora using the Kurucz and Atlas-3 SUSIM extraterrestrial spectrum are valid methods for measuring TCO.

[22] A small bias of approximately 2 DU (or, 0.6%) was found between the Brewer and Pandora TCO measurements that was constant with slant column (SC) ozone amount over the full range of solar zenith angles (15–80°) observed during our measurements (Figure 5). For the Pandora comparisons with the Brewer 6w-algorithm, scattering around this mean value of the bias was almost a constant ±10 DU (or ±3%), independent of the SC amount or solar zenith angle (Figure 5a). Comparisons with the Brewer Op-algorithm (Figure 5b) resulted in somewhat larger scattering around the mean value at small SC ozone amounts, as would be expected, since the additional use of the 2 shortest wavelengths (303 and 306 nm) in the 6w-retrieval improves the Brewer TCO estimates only at low SZAs or small SC (at high SZAs the 6w-algorithm is essentially reduced to the operational one).

[23] Solar zenith angle dependence resulted in 0.4% change in TCO differences over the observed SZA-range (15°–80°) for the comparison between Pandora and the Brewer 6w-algorithm and 1% change in TCO for the comparison with the Brewer Op-algorithm. Having the TCO differences almost independent of SZA (Figure 6) indicates that the stray-light method we applied to the Pandora measurements in the 310–330 nm region provided an adequate correction. However, the Brewer-Pandora differences showed some small seasonal dependence, with Pandora typically overestimating TCO during the winter months (square symbols in Figure 6) and underestimating TCO during the summer (circles in Figure 6). Average values of

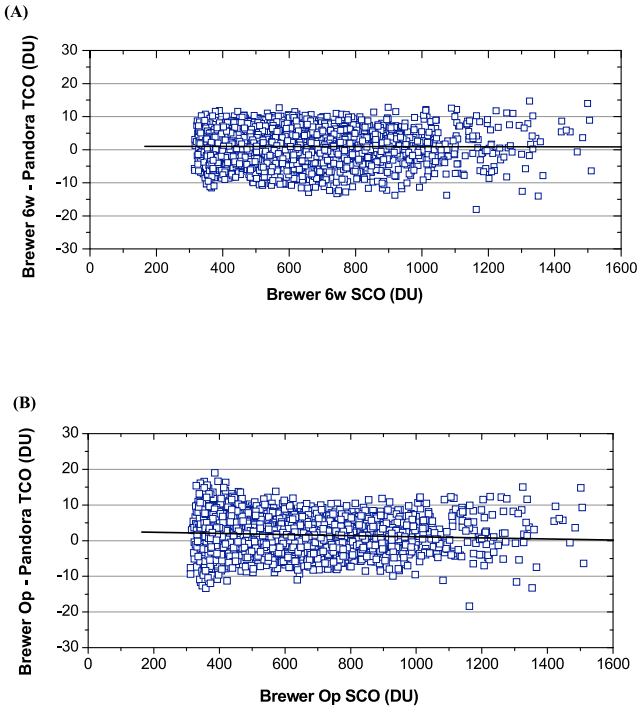

Figure 5. TCO residuals between Brewer and Pandora (instrument #9) as a function of Brewer Slant Column ozone (SCO), using (a) the 6-wavelength Brewer TCO algorithm and (b) the operational Brewer TCO algorithm. The practically zero slant column O_3 dependence suggests a negligible remaining stray light effect after the applied simple SL correction.

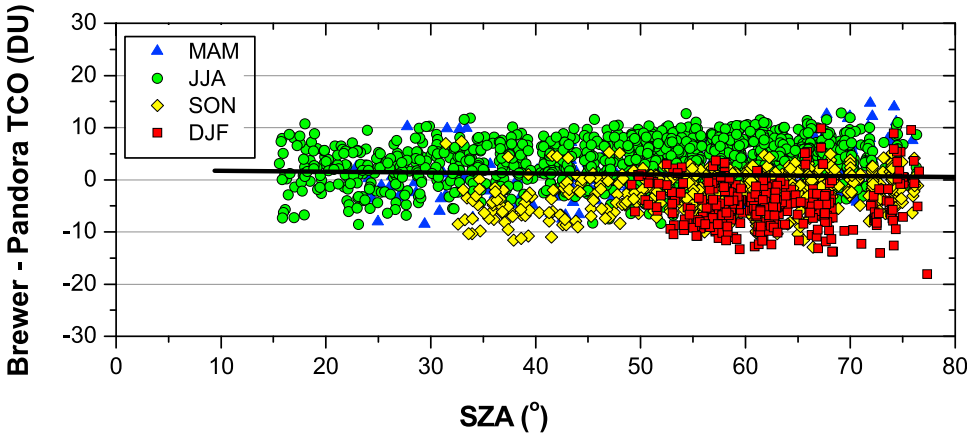

Figure 6. TCO residuals between Brewer (6w-algorithm) and Pandora (instrument #9) as a function of solar zenith angle (SZA). Results are shown in different symbols for different seasons (triangles for spring, MAM; circles for summer, JJA; diamonds for fall, SON; squares for winter, DJF). The liner regression on the data is shown as solid line and reflects the almost negligible SZA-dependence of the Brewer-Pandora residuals.

Brewer-Pandora differences were +3.6 DU (s.d. = 3.8 DU) or +1.15% during summer, and −4.74 DU (s.d. = 4.3 DU) or −1.32% during winter. Better agreement was observed during the spring and fall months with average TCO differences between the two instruments of 1.3 DU (s.d. = 4.2 DU) and 2.4 DU (s.d. = 3.6 DU), respectively. This small seasonal variability could be associated with the temperature dependence of the O_3 cross sections, assumed constant (T = 225°K) in our standard retrieval. Our sensitivity studies show that the retrieval of TCO has a temperature dependence of 1% per 3°K, with an underestimation in temperature (e.g., during summer) resulting in an underestimation of TCO values (i.e., positive Brewer-Pandora differences). Application of a temperature correction by approx. ±5°K, consistent with the TOMS version 8 temperature climatology for the specific latitude and TCO values [*McPeters et al.*, 2007], considerably reduces this small (<1.5%) seasonal dependence in TCO differences between the two instruments.

[24] Almost no SZA dependence was found for the comparison between the Brewer and Pandora instruments at the high-latitude site in Fairbanks, Alaska (Figures 4b, 8d) over the 58–80° SZA range observed by Brewer. TCO measurements were almost identical between the two Pandora instruments, the CMOS (#2) and CCD (#9) spectrometer systems (Figure 8d). Linear regression between Brewer and Pandora #2 resulted in a slope of 0.979 and strong correlation (R = 0.99). However, an offset of 16.55 DU was found between the two instruments, with Pandora systematically lower by 2–4% relative to the Brewer (Figures 4b and 8d). This is larger than the 2 DU offset found during the much longer GSFC Brewer-Pandora time series.

3.2. Comparison Between Pandora and Aura OMI

[25] Close agreement was found between Aura OMI and our ground-based measurements of TCO over all four study sites (Figures 7, 8, 10, 11). For comparisons with satellite observations, Brewer and Pandora data were averaged over a ±1-h window of the OMI overpass time. Ground-based measurements were filtered to only include data with uncertainty in TCO <2 DU and normalized RMS of weighted spectral fitting residuals <0.05. OMI data were filtered to keep only those data where the distance from GSFC was <50 km and the OMI radiative cloud-fraction was <0.2.

[26] Both Brewer and Pandora data agreed closely with the OMI near-overpass at GSFC, with an estimated slope not significantly different from 1 (1.001 and 1.009 respectively, Figures 7a and 7b). Both Pandora and Brewer slightly overestimated TCO relative to OMI by 0.7% and 0.3% respectively, with residuals in the range ±7%. Satellite and ground-based (Pandora or Brewer) TCO differences showed some dependence on OMI cross-track position (CTP) and the distance between the station and the OMI CTP, with the largest TCO differences (larger than 10%) associated in almost all cases and all sites with extreme CTP and distance from station larger than 25 km.

[27] Very good agreement between satellite and Pandora retrievals was also observed at Helsinki, Cabauw and Fairbanks (Figures 7c–7e), although the Pandora-OMI matchups were limited at these locations due to the shorter periods of ground-based instrument deployment. In all cases, linear regression between OMI and Pandora retrievals resulted in a slope close to 1 (0.95–1.02) and strong correlation coefficients (R within 0.97–0.99). Residuals between ground-based and satellite data at Cabauw ranged between ±2%, with an average difference between Pandora and OMI of just 0.3 DU (s.d. = 3 DU). Pandora underestimated TCO relative to OMI at Fairbanks, Alaska, on average by 1% (−4 DU average Pandora-OMI difference, s.d. = 5 DU), with TCO residuals between −12 and 3 DU. Differences between OMI and Pandora retrievals were within ±5% at the FMI station in Helsinki, Finland, with Pandora underestimating TCO, on average by 0.7% (Figures 7c–7e).

3.3. Temporal Variability in TCO From Pandora, Brewer, and OMI

[28] The frequent and continuous measurements by Pandora from sunrise to sunset allowed us to study temporal dynamics in ozone at our study sites (day-to-day and diurnal variation), and revealed short-term changes in TCO amounts

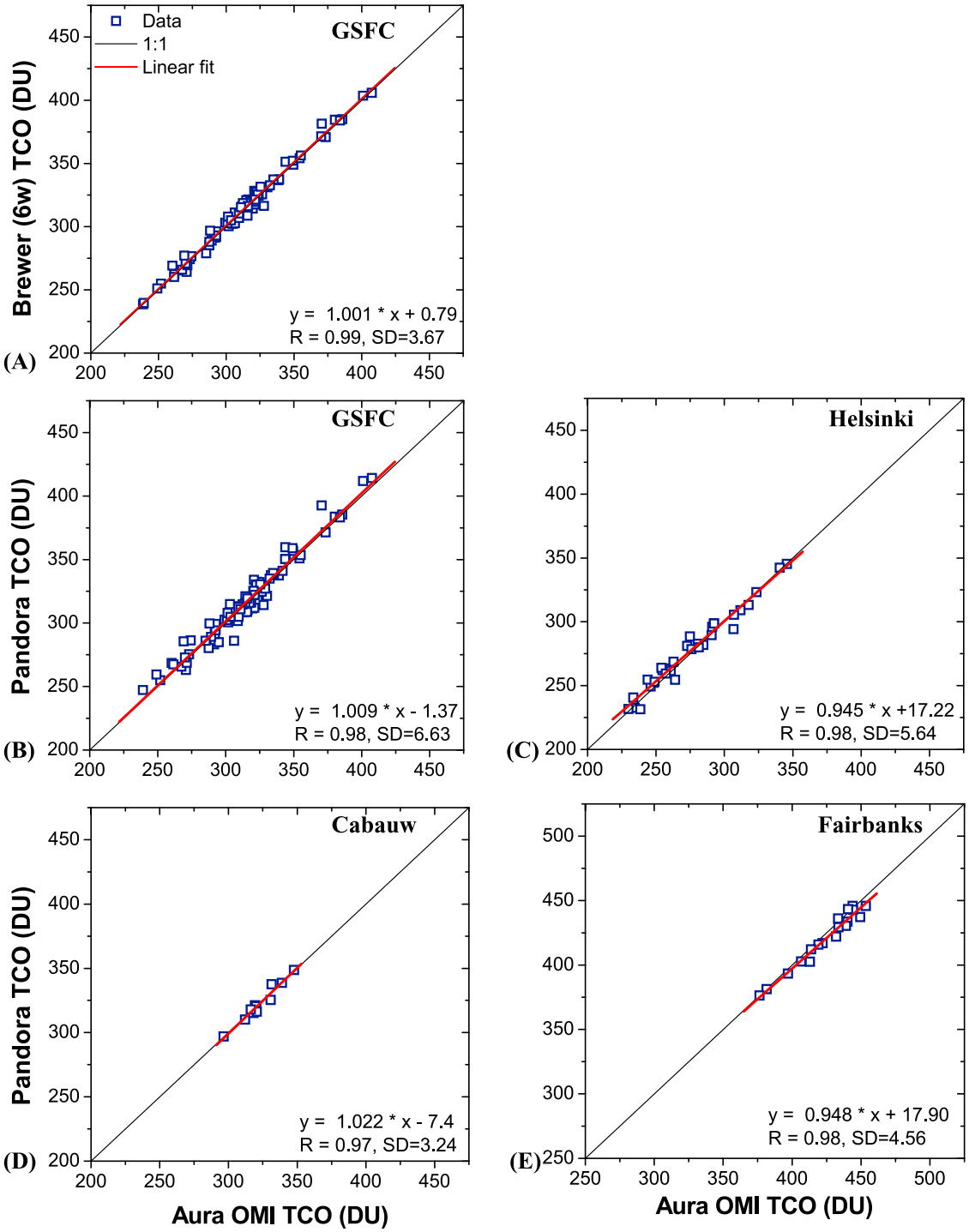

Figure 7. Comparison in TCO between AURA-OMI and (a) Brewer 6w-algorithm at the GSFC site (N = 90); (b) Pandora #9 at the GSFC site (N = 99); (c) Pandora #21 at Helsinki (N = 32); (d) Pandora #9 at Cabauw (N = 12); and (e) Pandora #9 at Fairbanks (N = 18) (similar results for Pandora #2 at Fairbanks). In all cases, P <0.0001.

not possible to capture by sun synchronous satellite observations, like Aura OMI, alone.

[29] Figure 8a shows comparisons between Pandora, Brewer and OMI over GSFC, for four example cases covering different seasons during the 2009–2010 period when Brewer and Pandora were collocated at GSFC. Similar comparisons between Pandora and OMI (and Brewer where available), are shown for Cabauw, Helsinki and Fairbanks in Figures 8b–8d, for four example cases covering the period of instrument deployment at these sites. In general, the diurnal TCO patterns depicted by our two ground-based instruments Pandora and Brewer were in very close agreement, both at GSFC and in Fairbanks, with few exceptions. On 4 May 2010, the morning data (9:00 to 11:00 UT) at GSFC show

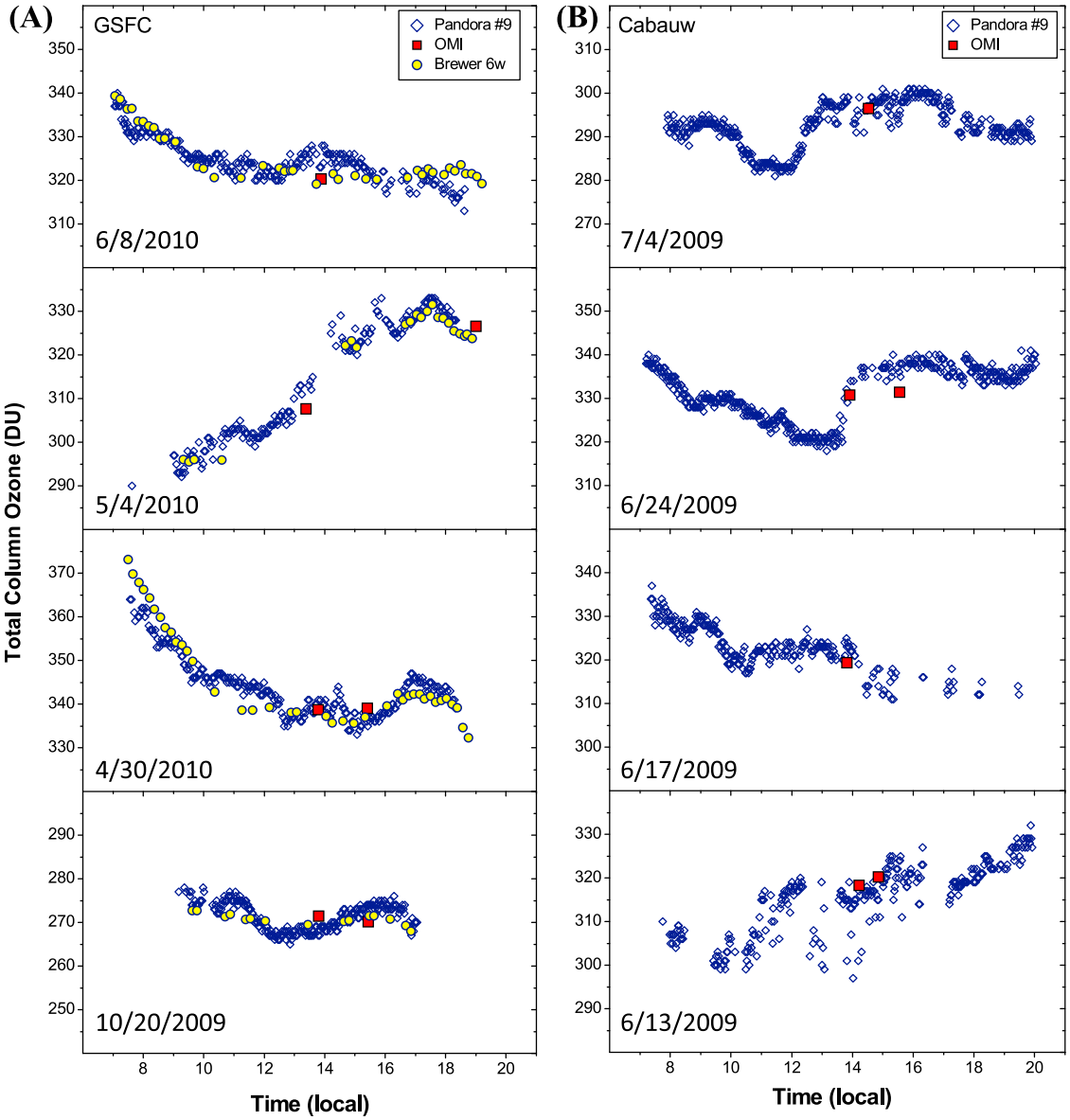

Figure 8. A comparison of total column ozone amounts between Pandora instruments (diamonds), Brewer 6w-algorithm (circles), and OMI (squares) at (a) GSFC, (b) Cabauw, (c) Helsinki, and (d) Fairbanks.

very good agreement. After that, the Brewer data become sparse, while the Pandora data remain at high precision. The usual reason for this type of behavior in the Brewer is that the aerosol variation was significant over the period (0.7 s) of the Brewer sequential wavelength measurement, causing significant O_3 variation between successive retrievals used in forming an average value (and standard error in estimated Brewer TCO > 2 DU). Aerosol variation has little effect on the Pandora TCO retrieval, plus Pandora can average more measurements together to minimize the noise in a single data point. Consistent with our results on the SZA-dependence of Brewer-Pandora TCO differences (discussed in section 3.1), the observed overall good agreement between the two instruments throughout the day suggests minimum residual stray light effects after stray light correction. This shows that Pandora can be used for satellite validation and ozone characterization under a wider variety of atmospheric conditions compared to the Brewer spectrometer, while being of comparable accuracy under clear-sky conditions.

[30] Variation in satellite retrieved total column ozone amounts over the approximately 1.5 h between two successive OMI orbits ranged from less than 1 DU (i.e., 24 June 2009, at Cabauw) to more than 19 DU (i.e., 4 May 2010, at Goddard) for the days shown in Figure 8. The large increase in TCO observed by OMI over GSFC on May 4th 2010 was also observed by Pandora and Brewer, indicating a real change in ozone amount. Such sharp (10–20 DU) spikes and dips in TCO have been observed in other days by both OMI successive overpasses and the higher resolution Pandora, and are mostly associated with changes in stratospheric

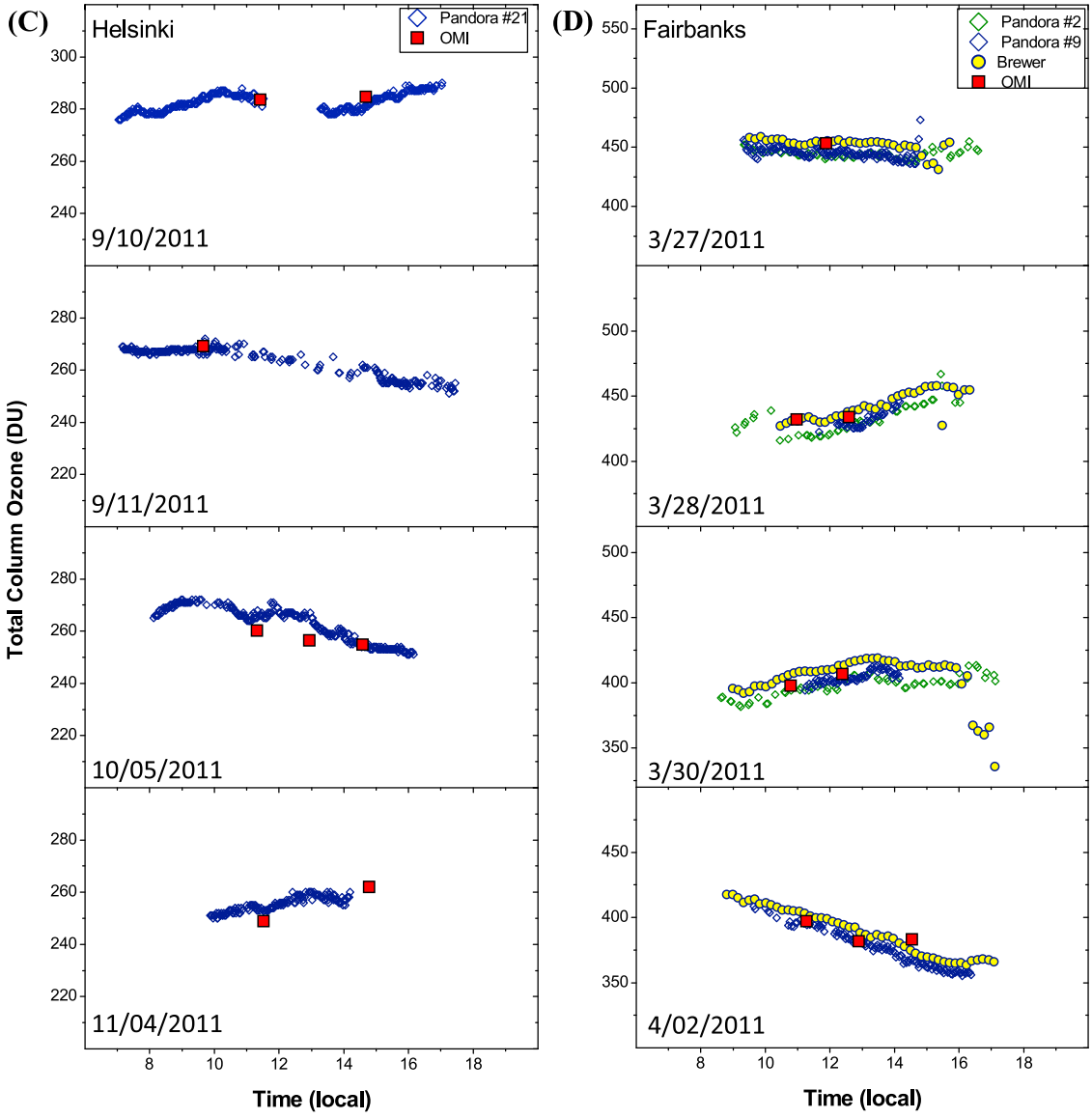

Figure 8. (continued)

ozone content due to weather systems (e.g., pressure changes, passage of a cold front with high ozone content, or intrusion of low-ozone air from lower latitudes). Aura-OMI observations of the ozone field over the Eastern U.S. on May 4th 2010 revealed that the sharp temporal change in TCO we observed at Goddard that day was indeed due to the passage of a front transporting air masses with higher TCO from the north to the south and over the GSFC area (Figure 9).

[31] Differences in retrieved TCO between two successive OMI overpasses, however, do not always reflect real changes in ozone content over a specific location, as this could also be the result of differences in the satellite FOV, large changes in distance between the station and the satellite cross-track position CTP (i.e., by more than 50 km), or rapid changes in cloud fraction and aerosols between the two overpasses. For example, on 27 April 2010 (data not shown here) the change in OMI retrieved TCO between two successive satellite overpasses at GSFC was as high as 47 DU, with a change in station-CTP distance, however, of more than 80 km. Both Brewer and Pandora at GSFC measured a change in TCO of less than 10 DU between the two OMI overpass times, suggesting a relatively large influence of horizontal atmospheric heterogeneity on the OMI TCO retrieval.

[32] For the cases shown in Figure 8, diurnal TCO variability as high as 40–50 DU was observed by our Pandora instruments (e.g., 30 April 2010 at GSFC, 2 April 2011 at Fairbanks). Such temporal changes in ozone occur occasionally at these mid- to high-latitude sites. An average amplitude of diurnal variation in TCO of 14 DU has been measured by Pandora over Goddard during the period May 2009–April 2011, while temporal changes as strong as 40 to 50 DU have been recorded on certain days by both Brewer and Pandora at this site. A diurnal variability of similar

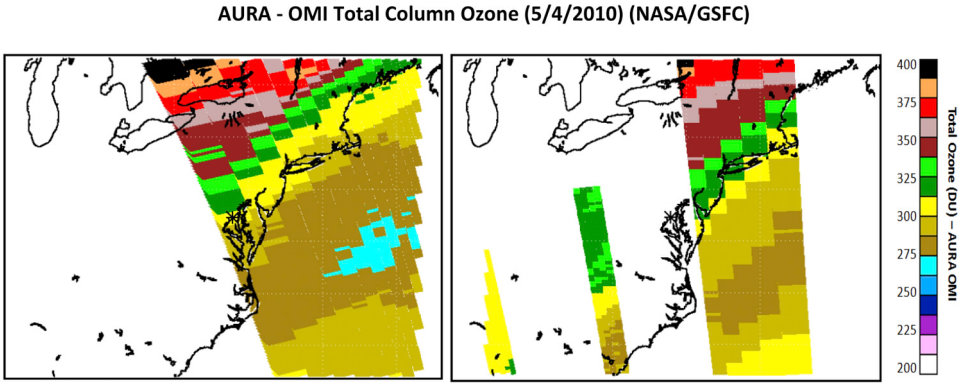

Figure 9. Aura-OMI TCO over the Eastern U.S. for two successive orbits on May 4, 2010 (orbits L2-OMTO3_2010m0504t1627-o30864_v003- 2012m0331t221500.he5 and_L2-OMTO3_2010m0504t1806-o30865_v003–2012m0331t221553.he5). The OMI images reveal the passage of a front moving from North to South and transporting air masses with higher TCO over the GSFC area. This spatial heterogeneity in TCO was reflected in the TCO time series measured during this day by both Brewer and Pandora at the GSFC site (see Figure 8a). Aura-OMI satellite images provided by Gordon Labow.

magnitude was observed in both Cabauw and Fairbanks, with an average change in TCO during the day of 16 DU and 20 DU, respectively. Diurnal variation with amplitude as strong as 25 to 30 DU was measured in several occasions over the 2 months (June–July) of the CINDI campaign. TCO changes as large as 30 to 46 DU were observed in Fairbanks, by both Brewer and Pandora during March 2011. Observed variability in TCO was lower at Helsinki, Finland, where average TCO change during the day was 12 DU during September to November 2011, with a maximum observed amplitude of diurnal variation of 33 DU. Observations at our high-latitude site in Helsinki during days when TCO remained almost constant throughout the day, revealed that the effect of stray light correction on the Pandora retrievals becomes apparent only at SZAs larger than 80 degrees (Figure 10). In terms of the slant optical path that includes total ozone dependent extinction, these results saw that Pandora TCO retrievals are accurate up to slant column ozone (SCO) amounts of 1,500 DU (=260 DU * AMF(80°), where AMF is the air mass factor). This is consistent with results at GSFC showing good agreement between Brewer and Pandora retrievals up to slant column ozone amounts of approximately 1,500 DU (Figure 5). Thus, in addition to the tight filtering of the data that removed all outliers (normalized root-mean square of weighted spectral fitting residuals less than 0.05 and estimated error in TCO less than 1 DU), measurements at SCO larger than 1500 DU were excluded for the above estimates of diurnal variability at our four study sites.

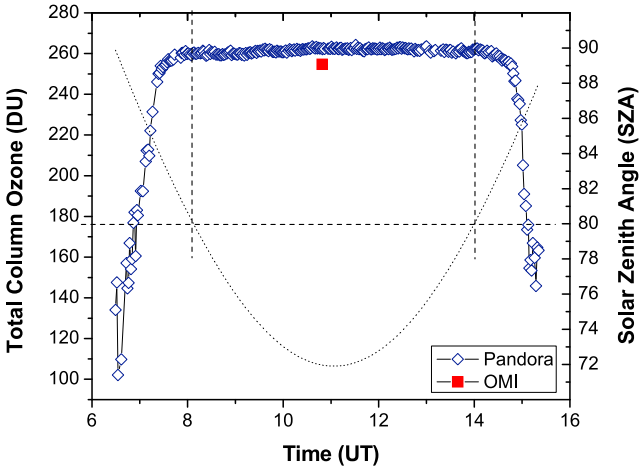

Figure 10. Comparison between Pandora (open diamonds) and OMI (filled square) for 24 October 2011, a typical day when TCO remained constant throughout the day, at the high latitude site Helsinki, in Finland (Lat = 60.2037°, Long = 24.9612°). The difference between Pandora and OMI TCO was 7.26 DU, or 2.8%. Pandora measurements are shown during the day (time on *x* axis and SZA on right *y* axis) The effect of residual stray light correction in Pandora becomes apparent only at SZAs larger than 80 degrees.

[33] The long time series of TCO measurements at Goddard was used to estimate seasonal variability in ozone at this midlatitude site (Figure 11). Estimates of monthly means

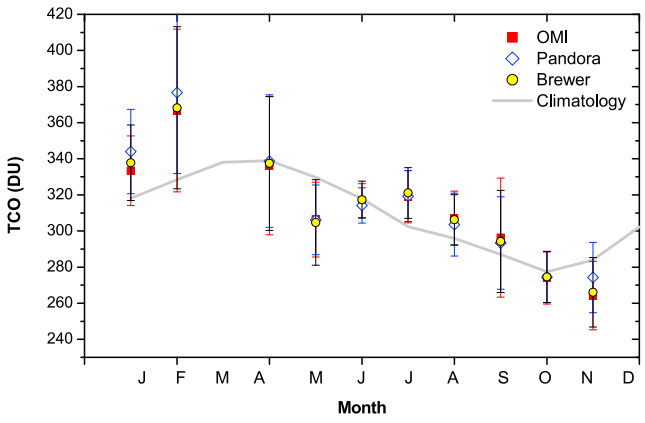

Figure 11. Mean monthly TCO values at GSFC measured by Brewer (circles), Pandora instrument #9 (diamonds) and OMI (squares). The TCO zonal-mean monthly mean climatology from OMI/MLS at 39° latitude [*Ziemke et al.*, 2011] is also shown for reference (gray line).

showed considerably higher ozone amounts and high variability during late winter and early spring, when monthly mean TCO was between 320 and 380 DU. A second smaller maximum was observed during July (~320 DU), possibly due to the particularly high tropospheric ozone amounts during summer in this area [*MDE*, 2008; *Ziemke et al.*, 2011]. Total column ozone dropped during the fall months, with monthly mean TCO in the range 275–300 DU. These results are consistent with the TCO zonal-mean monthly mean climatology derived from OMI and MLS (Microwave Limb Sounder) ozone measurements (2004–2010) at 39° latitude [*Ziemke et al.*, 2011]. Comparisons of TCO monthly averages between Pandora and OMI showed differences <6%, while Brewer and OMI showed differences <8%. Although these are observations at individual sites and over relative short time periods, Pandora measurements at our mid- to high- latitude sites (Cabauw at 54°N, Helsinki at 60°N and Fairbanks at 65°N) showed seasonal and latitudinal patterns in TCO that were generally in agreement with climatology. That is, an increase in TCO would be expected, based on climatology, with increasing latitude in the Northern Hemisphere, with higher values in early spring and lower values in fall [*Ziemke et al.*, 2011]. Total column ozone amounts were particularly high at our highest latitude site in Fairbanks Alaska (Figure 8). Monthly mean TCO was 426 DU (s.d. = 19 DU) in March and 420 DU (s.d. = 22 DU) in April 2011, approximately 10% higher than the 60–65° latitude monthly mean climatology from OMI and MLS. Total column ozone at the midlatitude Cabauw site during the CINDI campaign was on average 328 DU (s.d. = 15 DU) in June and 315 DU (s.d. = 17 DU) in July, very similar to the summer monthly TCO means at the midlatitude GSFC site. Lower ozone values were observed during fall 2011 in Helsinki, with monthly TCO of 284 DU (s.d. = 19 DU), 277 DU (s.d. = 31 DU), and 257 DU (s.d. = 14 DU), in September, October and November, respectively, consistent with TCO climatology in the 55–65° latitude zone.

4. Summary

[34] The Pandora and Brewer TCO measurements at the GSFC site were found to be in close agreement (0.6% bias) throughout the day, including near sunrise and sunset conditions with solar zenith angles up to 80°, or SCO amounts up to 1,500 DU. The good agreement in accuracy over a wide range of ozone values (240–490 DU) suggests that the Brewer transferred Mauna Loa calibration and the absolute calibration of Pandora using a combination of the independently measured Atlas-3 SUSIM and Kurucz extraterrestrial spectra are in good agreement. The practically negligible SZA dependence of the TCO residuals between Pandora and the well-calibrated double grating Brewer spectrometer #171 that was observed at both GSFC and Fairbanks and for both Pandora CMOS (#2) and CCD (#9) systems, shows that the stray-light correction method applied to Pandora provided an adequate correction. This successful ground-based instrument intercomparison suggests that the Pandora direct-sun spectral fitting technique can be reliably used for satellite validation (e.g., Aura-OMI and NPP-OMPS), and can be applied to characterization of total column ozone dynamics under a wider variety of atmospheric conditions compared to direct sun observations from the Brewer spectrometer, while being comparable under clear-sky conditions. Zenith sky observations from both instruments could further extend TCO retrievals under cloudy conditions [*Fioletov et al.*, 2011]. Pandora and Aura-OMI TCO retrievals were found to be in very good agreement across all sites, GSFC, Cabauw, Helsinki and Fairbanks, when the OMI cross track position was at a distance of less than 50 km from the Pandora location, and OMI-measured cloud fraction was less than 0.2. In all cases, linear regression between OMI and Pandora retrievals resulted in a slope close to 1 (0.95–1.02) and strong correlation coefficients (R within 0.97–0.99). Residuals between ground-based and satellite data ranged between ±7%, with Pandora slightly overestimating TCO at GSFC (by 0.7%), while slightly underestimating TCO at Fairbanks (1%) and Helsinki (0.7%).

[35] Our Pandora ground-based measurements at four sites extending from 39°N to 65°N latitude, revealed seasonal and latitudinal patterns in TCO that were generally in agreement with OMI-MLS climatology. Overall, we observed increasing TCO with increasing latitude, with higher values in early spring and lower values in fall. A second smaller maximum was observed during July at GSFC, most likely associated with the particularly high tropospheric ozone amounts typically observed in this area during summer. Considerable diurnal variability, on some days as high as 40 to 50 DU, was capture by the frequent and continuous Pandora measurements at these mid- to high- latitude sites. Short-term (hourly) temporal changes in ozone amounts cannot always be captured by OMI or other satellite instruments in sun-synchronous orbits with 1 to 3 daily overpasses. Such a variation in TCO, of the order of 10 to 15%, is especially important if it involves an ozone reduction near noon hours, since it causes a 10 to 15% increase in erythemal UV irradiance, which is an important factor in human health. Such variations are not usually included in the UV index forecast.

References

Bais, A. F. (1997), Absolute spectral measurements of direct solar ultraviolet irradiance with a Brewer spectrophotometer, *Appl. Opt.*, *36*, 5199–5204, doi:10.1364/AO.36.005199.

Bass, A. M., and R. J. Paur (1985), The ultraviolet cross-sections of ozone, I, The measurements, in *Atmospheric Ozone: Proceedings of the Quadrennial Ozone Symposium*, edited by C. S. Zerefos and A. Ghazi, pp. 606–616, D. Reidel, Dordrecht, Netherlands.

Bernhard, G., C. R. Booth, and J. C. Ehramjian (2004), Version 2 data of the National Science Foundation's ultraviolet radiation monitoring network: South Pole, *J. Geophys. Res.*, *109*, D21207, doi:10.1029/2004JD004937.

Bhartia, P. K., R. D. McPeters, C. L. Mateer, L. E. Flynn, and C. Wellemeyer (1996), Algorithm for the estimation of vertical ozone profiles from the backscattered ultraviolet technique, *J. Geophys. Res.*, *101*(D13), 18,793–18,806, doi:10.1029/96JD01165.

Bovensmann, H., J. P. Burrows, M. Buchwitz, J. Frerick, S. Noel, V. V. Rozanov, K. V. Chance, and A. P. H. Goede (1999), SCIAMACHY: Mission objectives and measurement modes, *J. Atmos. Sci.*, *56*(2), 127–150, doi:10.1175/1520-0469(1999)056<0127:SMOAMM>2.0.CO;2.

Brasseur, G. P., J. T. Kiehl, J.-F. Mueller, T. Schneider, C. Granier, X. X. Tie, and D. Hauglustaine (1998), Past and future changes in global tropospheric ozone: Impact on radiative forcing, *Geophys. Res. Lett.*, *25*, 3807–3810, doi:10.1029/1998GL900013.

Burrows, J. P., et al. (1999), The global ozone monitoring experiment (GOME): Mission concept and first scientific results, *J. Atmos. Sci.*, *56*(2), 151–175, doi:10.1175/1520-0469(1999)056<0151:TGOMEG>2.0.CO;2.

Carpenter, L. J., P. S. Monks, B. J. Bandy, and S. A. Penkett (1997), A study of peroxy radicals and ozone photochemistry at coastal sites in the northern and southern hemispheres, *J. Geophys. Res.*, *102*(D21), 25,417–25,427, doi:10.1029/97JD02242.

Cede, A., S. Kazadzis, M. Kowalewski, A. Bais, N. Kouremeti, M. Blumthaler, and J. Herman (2006a), Correction of direct irradiance measurements of

Brewer spectrophotometers due to the effect of internal polarization, *Geophys. Res. Lett.*, *33*, L02806, doi:10.1029/2005GL024860.
Cede, A., J. R. Herman, A. Richter, N. Krotkov, and J. Burrows (2006b), Measurements of nitrogen dioxide total column amounts using a Brewer double spectrometer in direct Sun mode, *J. Geophys. Res.*, *111*, D05304, doi:10.1029/2005JD006585.
Chameides, W. L. (1978), The photochemical role of tropospheric nitrogen oxides, *Geophys. Res. Lett.*, *5*, 17–20, doi:10.1029/GL005i001p00017.
Chameides, W. L., P. S. Kasibhatla, J. Yienger, and H. Levy (1994), Growth of continental scale MetroAgroPlexes, regional ozone pollution and world food production, *Science*, *264*, 74–77, doi:10.1126/science.264.5155.74.
Comrie, A. C., and B. Yarnal (1992), Relationships between synoptic-scale atmospheric circulation and ozone concentrations in metropolitan Pittsburgh, Pennsylvania, *Atmos Environ., Part B*, *26*, 301–312.
Crutzen, P. J. (1995), Ozone in the troposphere, in *Composition, Chemistry and Climate of the Atmosphere*, edited by H. B. Singh, pp. 349–393, Van Nostrand Reinhold, New York.
Crutzen, P. J., M. G. Lawrence, and U. Poschl (1999), On the background photochemistry of tropospheric ozone, *Tellus, Ser. A*, *51*, 123–146, doi:10.1034/j.1600-0870.1999.t01-1-00010.x.
Daumont, M., J. Brion, J. Charbonnier, and J. Malicet (1992), Ozone UV spectroscopy, I: Absorption cross-sections at room temperature, *J. Atmos. Chem.*, *15*, 145–155, doi:10.1007/BF00053756.
David, L. M., and P. R. Nair (2011), Diurnal and seasonal variability of surface ozone and NOx at a tropical coastal site: Association with mesoscale and synoptic meteorological conditions, *J. Geophys. Res.*, *116*, D10303, doi:10.1029/2010JD015076.
De Bock, V., H. De Backer, A. Mangold, and A. Delcloo (2010), Aerosol optical depth measurements at 340 nm with a Brewer spectrophotometer and comparison with Cimel sunphotometer observations at Uccle, Belgium, *Atmos. Meas. Tech.*, *3*, 1577–1588, doi:10.5194/amt-3-1577-2010.
Diffey, B. L. (1991), Solar ultraviolet radiation effects on biological systems, *Phys. Med. Biol.*, *36*, 299–328, doi:10.1088/0031-9155/36/3/001.
Dobson, G. M. B. (1957), Observers handbook for the ozone spectrophotometer, *Ann. Int. Geophys. Year*, *5*(1), 46–89.
Dueñas, C., M. C. Fernández, S. Cañete, J. Carretero, and E. Liger (2002), Assessment of ozone variations and meteorological effects in an urban area in the Mediterranean coast, *Sci. Total Environ.*, *299*, 97–113, doi:10.1016/S0048-9697(02)00251-6.
Environmental Protection Agency (1998), National air quality and emissions trends report 1998, *Rep. EPA 454/R-00-003*, U.S. Environ. Prot. Agency, Research Triangle Park, N. C.
Fioletov V. E., C. A. McLinden, C. T. McElroy, and V. Savastiouk (2011), New method for deriving total ozone from Brewer zenith sky observations, *J. Geophys. Res.*, *116*, D08301, doi:10.1029/2010JD015399.
Fioletov, V. E., E. Griffioen, J. B. Kerr, D. I. Wardle, and O. Uchino (1998), Influence of volcanic sulfur dioxide on spectral UV irradiance as measured by Brewer spectrophotometers, *Geophys. Res. Lett.*, *25*, 1665–1668, doi:10.1029/98GL51305.
Fioletov, V. E., J. B. Kerr, C. T. McElroy, D. I. Wardle, V. Savastiouk, and T. S. Grajnar (2005), The Brewer reference triad, *Geophys. Res. Lett.*, *32*, L20805, doi:10.1029/2005GL024244.
Fishman, J., S. Solomon, and P. Crutzen (1979), Observational and theoretical evidence in support of tropospheric ozone, *Tellus*, *31*, 432–446, doi:10.1111/j.2153-3490.1979.tb00922.x.
Gröbner, J., and J. B. Kerr (2001), Ground-dased determination of ultraviolet extraterrestrial solar irradiance: Providing a link between space-based and ground-based solar UV measurements, *J. Geophys. Res.*, *106*(D7), 7211–7217, doi:10.1029/2000JD900756.
Heck, W. W., O. C. Taylor, R. Adams, G. Bingham, J. Miller, E. Preston, and L. Weinstein (1982), Assessment of crop loss from ozone, *J. Air Pollut. Control Assoc.*, *32*, 353–361, doi:10.1080/00022470.1982.10465408.
Herman, J. R., A. Cede, E. Spinei, G. Mount, M. Tzortziou, and N. Abuhassan (2009), NO_2 column amounts from ground-based Pandora and MFDOAS spectrometers using the direct-sun DOAS technique: Intercomparisons and application to OMI validation, *J. Geophys. Res.*, *114*, D13307, doi:10.1029/2009JD011848.
Herman, J. R. (2010), Use of an improved radiation amplification factor to estimate the effect of total ozone changes on action spectrum weighted irradiances and an instrument response function, *J. Geophys. Res.*, *115*, D23119, doi:10.1029/2010JD014317.
Intergovernmental Panel on Climate Change (2007), *Climate Change 2007: The Physical Science Basis, Contribution of Working Group I to the Fourth Assessment Report of the Intergovernmental Panel on Climate Change*, edited by S. Solomon et al., Cambridge Univ. Press, Cambridge, U. K.
Kerr, J. B. (2002), New methodology for deriving total ozone and other atmospheric variables from Brewer spectrophotometer direct sun spectra, *J. Geophys. Res.*, *107*(D23), 4731, doi:10.1029/2001JD001227.
Kerr, J. B., C. T. McElroy, and R. A. Olafson (1981), Measurements of ozone with the Brewer spectrophotometer, in *Proceedings of the Quadrennial Ozone Symposium*, edited by J. London, pp. 74–79, Nat. Cent. for Atmos. Res., Boulder, Colo.
Kerr, J. B., C. T. McElroy, D. I. Wardle, R. A. Olafson, and W. F. J. Evans (1985), The automated Brewer spectrophotometer, in *Atmospheric Ozone: Proceedings of the Quadrennial Ozone Symposium*, edited by C. S. Zerefos and A. Ghazi, pp. 396–401, D. Reidel, Dordrecht, Netherlands.
Kerr, J. B., I. A. Asbridge, and W. F. J. Evans (1988), Intercomparison of total ozone measured by the Brewer and Dobson spectrophotometers at Toronto, *J. Geophys. Res.*, *93*, 11,129–11,140, doi:10.1029/JD093iD09p11129.
Kurucz, R. L. (2005), New atlases for solar flux, irradiance, central intensity, and limb intensity, paper presented at the ATLAS12 and related codes workshop, Trieste Astron. Obs., Trieste, Italy, 11–15 July.
Lakkala, K., et al. (2008), Quality assurance of the Brewer spectral UV measurements in Finland, *Atmos. Chem. Phys.*, *8*, 3369–3383, doi:10.5194/acp-8-3369-2008.
Lehman, J., K. Swinton, S. Bortnick, C. Hamilton, E. Baldridge, B. Eder, and B. Cox (2004), Spatio-temporal characterization of tropospheric ozone across the eastern United States, *Atmos. Environ.*, *38*, 4357–4369, doi:10.1016/j.atmosenv.2004.03.069.
Levy, H., II (1971), Normal atmosphere: Large radical and formaldehyde concentrations predicted, *Science*, *173*, 141–143, doi:10.1126/science.173.3992.141.
Logan, J. A., J. J. Prather, S. C. Wofsy, and M. B. McElroy (1981), Tropospheric chemistry: A global perspective, *J. Geophys. Res.*, *86*, 7210–7254, doi:10.1029/JC086iC08p07210.
Loyola, D., R. M. Coldewey-Egbers, M. Dameris, H. Garny, A. Stenke, M. Van Roozendael, C. Lerot, D. Balis, and M. Koukouli (2009), Global long-term monitoring of the ozone layer—A prerequisite for predictions, *Int. J. Remote Sens.*, *30*(15), 4295–4318, doi:10.1080/01431160902825016.
Maryland Department of the Environment (MDE) (2008), Air quality seasonal report: Ground-level ozone, report, Baltimore, Md.
McPeters, R. D., G. J. Labow, and J. A. Logan (2007), Ozone climatological profiles for satellite retrieval algorithms, *J. Geophys. Res.*, *112*, D05308, doi:10.1029/2005JD006823.
McPeters, R., M. Kroon, G. Labow, E. Brinksma, D. Balis, I. Petropavlovskikh, J. P. Veefkind, P. K. Bhartia, and P. F. Levelt (2008), Validation of the Aura Ozone Monitoring Instrument total column ozone product, *J. Geophys. Res.*, *113*, D15S14, doi:10.1029/2007JD008802.
Noxon, J. F. (1975), Nitrogen dioxide in stratosphere and troposphere measured by ground based absorption spectroscopy, *Science*, *189*, 547–549, doi:10.1126/science.189.4202.547.
Petropavlovskikh, R. Evans, G. McConville, S. Oltmans, D. Quincy, K. Lantz, P. Disterhoft, M. Stanek, and L. Flynn (2011), Sensitivity of Dobson and Brewer Umkehr ozone profile retrievals to ozone cross-sections and stray light effects, *Atmos. Meas. Tech.*, *4*, 1841–1853, doi:10.5194/amt-4-1841-2011.
Piters, A. J. M., et al. (2012), The Cabauw intercomparison campaign for nitrogen dioxide measuring instruments (CINDI): Design, execution, and early results, *Atm. Meas. Tech.*, *5*, 457–485, doi:10.5194/amt-5-457-2012.
Platt, U., D. Perner, and H. W. Pätz (1979), Simultaneous measurement of atmospheric CH_2O, O_3, and NO_2 by differential optical absorption, *J. Geophys. Res.*, *84*, 6329–6335, doi:10.1029/JC084iC10p06329.
Redondas, A., and A. Cede (2006), Brewer algorithm sensitivity analysis, paper presented at the SAUNA workshop, SCIAMACHY, Puerto de la Cruz, Spain, 8 Nov.
Reich, P. B., and R. G. Amundson (1985), Ambient levels of ozone reduce net photosynthesis in tree and crop species, *Science*, *230*, 566–570, doi:10.1126/science.230.4725.566.
Roscoe, H. K., et al. (2010), Intercomparison of slant column measurements of NO_2 and O_4 by MAX-DOAS and zenith-sky UV and visible spectrometers, *Atmos. Meas. Tech.*, *3*, 1629–1646, doi:10.5194/amt-3-1629-2010.
Solomon, S. (1999), Stratospheric ozone depletion: A review of concepts and history, *Rev. Geophys.*, *37*, 275–316, doi:10.1029/1999RG900008.
Tevini, M. (1993), Effects of enhanced UV-B radiation on terrestrial plants, in *UV-B Radiation and Ozone Depletion: Effects on Humans, Animals, Plants, Microorganisms, and Materials*, edited by M. Tevini, pp. 125–153, Lewis, Boca Raton, Fla.
Thuillier, G., M. Herse, D. Labs, T. Foujols, W. Peetermans, D. Gillotay, P. C. Simon, and H. Mandel (2003), The solar spectral irradiance from 200 to 2400 nm as measured by the SOLSPEC spectrometer form the ATLAS and EURECA missions, *Sol. Phys.*, *214*, 1–22, doi:10.1023/A:1024048429145.

Tu, J., Z. G. Xia, H. Wang, and W. Li (2007), Temporal variations in surface ozone and its precursors and meteorological effects at an urban site in China, *Atmos. Res.*, *85*, 310–337, doi:10.1016/j.atmosres.2007.02.003.

Tzortziou, M., N. A. Krotkov, A. Cede, J. R. Herman, and A. Vassilkov (2008), A new technique for retrieval of tropospheric and stratospheric ozone profiles using sky radiance measurements at multiple view angles: Application to a Brewer spectrometer, *J. Geophys. Res.*, *113*, D06304, doi:10.1029/2007JD009093.

Veefkind, J. P., and J. F. de Haan (2002), DOAS total O3 algorithm, in *OMI Algorithm Theoretical Basis Document*, vol. 2, *OMI Ozone Products, Rep. ATBD-OMI-02*, edited by P. K. Barthia, pp. 33–52, NASA Goddard Space Flight Cent., Greenbelt, Md.

World Health Organization (2000), *Guidelines for Air Quality*, 190 pp., Geneva, Switzerland.

World Meteorological Organization (2006), Scientific assessment of ozone depletion: 2006, WMO Global Ozone Research and Monitoring Project, *Rep. 50*, Geneva, Switzerland.

Zerefos, C., G. Contopoulos, and G. Skalkeas (Eds.) (2009), *Twenty Years of Ozone Decline: Proceedings of the Symposium for the 20th Anniversary of the Montreal Protocol*, Springer, Dordrecht, Netherlands.

Zieger, P., et al. (2011), Comparison of ambient aerosol extinction coefficients obtained from in-situ, MAX-DOAS and LIDAR measurements at Cabauw, *Atmos. Chem. Phys.*, *11*, 2603–2624, doi:10.5194/acp-11-2603-2011.

Ziemke, J. R., S. Chandra, G. J. Labow, P. K. Bhartia, L. Froidevaux, and J. C. Witte (2011), A global climatology of tropospheric and stratospheric ozone derived from Aura OMI and MLS measurements, *Atmos. Chem. Phys.*, *11*, 9237–9251, doi:10.5194/acp-11-9237-2011.